Manuscript under review for journal Atmos. Meas. Tech.

Discussion started: 22 May 2018

© Author(s) 2018. CC BY 4.0 License.





1 2		18 May 2018			
3					
4					
5 6					
7		rntion cross sections for			
8					
9					
	10				
	11 by				
	12				
13	Jeremy J. Harriso	$n^{1,2,3}$			
14	14				
15	¹ Department of Physics and Astronomy, University	¹ Department of Physics and Astronomy, University of Leicester, Leicester LE1 7RH, United			
16	16 Kingdom.	Kingdom.			
17	17 ² National Centre for Earth Observation, University	² National Centre for Earth Observation, University of Leicester, Leicester LE1 7RH, United			
18	18 Kingdom.				
19	19 ³ Leicester Institute for Space and Earth Observation	ı, University of Leicester, Leicester LEI			
20	20 7RH, United Kingdom.				
21	21				
22	Number of pages = 18				
	Number of tables $= 3$				
24	Number of figures = 5				
	25				
	26 27 Address for correspondence:				
	28				
29	Dr. Jeremy J. Harrison				
	National Centre for Earth Obse				
31		tronomy			
32 33					
34					
35					
	36				
37	37 <i>e-mail</i> : jh592@leicester.ac.uk				
20	38				

Manuscript under review for journal Atmos. Meas. Tech.

Discussion started: 22 May 2018

© Author(s) 2018. CC BY 4.0 License.





Abstract

Trichlorofluoromethane (CFC-11), a widely used refrigerant throughout much of the twentieth century and a very potent (stratospheric) ozone depleting substance (ODS), is now banned under the Montreal Protocol. With a long atmospheric lifetime, it will only slowly degrade in the atmosphere, so monitoring its vertical concentration profile using infrared-sounding instruments, thereby validating stratospheric loss rates in atmospheric models, is of great importance; this in turn requires high quality laboratory spectroscopic data.

This work describes new high-resolution infrared absorption cross sections of trichlorofluoromethane / dry synthetic air over the spectral range 710 – 1290 cm⁻¹, determined from spectra recorded using a high-resolution Fourier transform spectrometer (Bruker IFS 125HR) and a 26-cm-pathlength cell. Spectra were recorded at resolutions between 0.01 and 0.03 cm⁻¹ (calculated as 0.9/MOPD; MOPD = maximum optical path difference) over a range of temperatures and pressures (7.5 – 760 Torr and 192 – 293 K) appropriate for atmospheric conditions. This new cross-section dataset improves upon the one currently available in the HITRAN and GEISA databases.

Manuscript under review for journal Atmos. Meas. Tech.

Discussion started: 22 May 2018







1. Introduction

Chlorofluorocarbons (CFCs) were first developed in the 1930s as safe, reliable, and non-toxic refrigerants for domestic use. Trichlorofluoromethane, known as CFC-11 or Freon-11, and dichlorodifluoromethane, known as CFC-12 or Freon-12, were the two most widely used CFCs in applications ranging from refrigerators and air conditioners to propellants in spray cans and blowing agents in foam production.

Ultimately, however, CFCs proved too good to be true. The explosion in their use led to a steady increase in their atmospheric abundances. While inert in the troposphere, it was this stability which enabled them to reach the stratosphere where dissociation by ultraviolet radiation released chlorine atoms, which catalyse the destruction of stratospheric ozone. The realisation of this impending environmental disaster prompted international action and in 1987 the Montreal Protocol was ratified; this led to the phasing out of the worldwide production and use of CFCs. CFCs are still released into the atmosphere from "banks", such as old refrigerators, however these are not regulated by the Protocol (Harris et al., 2014). Banks are the major source of emissions for many ODSs, including CFC-11 which has a long atmospheric lifetime of 52 years (Harris et al., 2014).

At present, CFC-11 is the second most abundant CFC in the atmosphere and contributes the second-highest amount of chlorine to the stratosphere, behind CFC-12. In addition to its role in stratospheric ozone destruction – it has the highest ozone depletion potential (1.0) (Harris et al., 2014) of all the CFCs – CFC-11 is a particularly strong greenhouse gas – it has a 100-yr global warming potential of 5160 (Harris et al., 2014).

As a key species in stratospheric ozone destruction, CFC-11 atmospheric concentrations are monitored in situ at the surface, e.g. the annual global mean mole fraction of CFC-11 measured by the AGAGE (Advanced Global Atmospheric Gases Experiment) network in 2012 was 235.5 ppt (Carpenter et al., 2014). However, in order to measure concentrations in the stratosphere where ozone destruction occurs, remote-sensing techniques are required. Table 1 contains a listing of limb sounders capable of measuring CFC-11, as described in the literature.

The infrared (IR) spectra for large molecules like trichlorofluoromethane are highly complex, consisting of very many closely spaced spectroscopic lines, making the task of generating line parameters from measurements an almost impossible one. For the purposes of atmospheric remote sensing, it is possible to use absorption cross sections in forward models instead of line parameters, however this requires laboratory measurements of air-broadened spectra over a range of temperatures and pressures. The accuracy of retrievals of

Manuscript under review for journal Atmos. Meas. Tech.

Discussion started: 22 May 2018

© Author(s) 2018. CC BY 4.0 License.





CFC-11 abundances for the limb sounders in Table 1 is very much dependent on the quality of the underlying spectroscopy; ideally absorption cross-section datasets should cover a range of atmospherically relevant pressure-temperature (PT) combinations, with accurate wavenumber scales and band intensities, and properly resolved spectral features. This work presents new spectroscopic data, optimised for limb sounding instruments, which improve upon those currently available in the HITRAN and GEISA databases.

2. Infrared spectroscopy of trichlorofluoromethane

2.1. Spectroscopic background

There are two stable isotopes of carbon and chlorine, and one of fluorine, resulting in eight stable isotopologues of trichlorofluoromethane, namely $^{12/13}C^{35}Cl_3F$, $^{12/13}C^{35}Cl_2^{37}Cl_5F$, $^{12/13}C^{35}Cl_3^{37}Cl_3F$; these belong to the point groups C_{3v} , C_s , C_s and C_{3v} , respectively. Taking into account the natural abundances of ^{12}C / ^{13}C (~ 99% and ~1%), and ^{35}Cl / ^{37}Cl (~ 76% and ~24%), the most abundant isotopologues are therefore $^{12}C^{35}Cl_3F$, $^{12}C^{35}Cl_3^{37}Cl_5F$, and $^{12}C^{35}Cl_3^{37}Cl_5F$, with abundances of 43%, 41%, and 13%, respectively.

As a non-linear molecule with five atoms, trichlorofluoromethane possesses nine normal vibrational modes; in the C_{3v} point group there are three non-degenerate fundamentals of A_1 symmetry (v_1 , v_2 , and v_3), and three doubly-degenerate fundamentals of E_3 symmetry (v_4 , v_5 , and v_6). For the E_3 point group, the E_3 , and E_3 modes possess E_3 symmetry, with the doubly-degenerate E_4 , E_5 , and E_6 modes each splitting into one E_3 and one E_3 mode (Snels et al., 2001). Since the splittings in the E_4 , E_5 , and E_6 levels are small, it is normal to label these bands assuming E_3 symmetry. The 710 – 1290 cm⁻¹ spectral range covered in the present work contains two strong fundamental bands, E_5 cm⁻¹, and a weaker combination band, E_7 and E_7 modes for the most abundant isotopologue, E_7 from Lilienfeld et al., 2007; Snels et al., 2001). Isotopologues complicate the already dense E_7 from Lilienfeld et al., 2007; Snels et al., 2001). Isotopologues complicate the already dense E_7 from Lilienfeld by small amounts relative to each other. These main band systems are shown in Figure 1 in the plot of the new absorption cross section at 191.7 K and 7.535 Torr. Details on the measurement conditions and derivation of this cross section are given in Section 3.

2.2. A brief history of trichlorofluoromethane absorption cross sections

High resolution (0.03 cm⁻¹) absorption cross sections of pure trichlorofluoromethane at 296 K were first included in HITRAN as part of the 1986 compilation (Massie et al., 1985;

Manuscript under review for journal Atmos. Meas. Tech.

Discussion started: 22 May 2018

© Author(s) 2018. CC BY 4.0 License.





Rothman et al., 1987). The HITRAN 1991/1992 compilation saw the first introduction of temperature-dependent cross sections (203 – 293 K) for CFC-11 (McDaniel et al., 1991; Rothman et al., 1992; Massie and Goldman, 1992); as before these were derived from measurements of pure CCl₃F at 0.03 cm⁻¹ resolution.

While the two previous HITRAN editions (1986 and 1991/1992) neglected pressure-broadening effects on the CCl₃F spectra, cross sections for 33 distinct PT combinations (201–296 K and 40–760 Torr N₂-broadened) over two wavenumber ranges, 810–880 cm⁻¹ and 1050–1120 cm⁻¹, were introduced into HITRAN 1996 (Li and Varanasi, 1994; Rothman et al., 1998). Another 22 PT combinations covering lower pressures and temperatures over the same wavenumber ranges were added to HITRAN 2000 (provided by Varanasi, cited within Rothman et al., 2003), bringing the overall PT coverage to 190–296 K and 8–760 Torr. Out of these 55 PT combinations, four pairs possess both temperature and pressure within 1 K and 5 Torr, respectively. This dataset, henceforth referred to as the Varanasi dataset, has been used widely for remote-sensing applications since it was first introduced; it is still the dataset included in the most recent GEISA 2015 (Jacquinet-Husson et al., 2016) and HITRAN 2016 (Gordon et al., 2017) spectroscopic databases. Despite its widespread use, the Varanasi dataset has some deficiencies which will be discussed in Section 4, alongside a comparison with the new spectroscopic data taken as part of the present work.

3. New absorption cross sections of air-broadened trichlorofluoromethane

3.1. Experimental

The experimental setup at the Molecular Spectroscopy Facility (MSF), Rutherford Appleton Laboratory (RAL) and the experimental procedures have been described previously for related measurements (e.g. Harrison et al., 2010; Harrison, 2015b; Harrison, 2016); the reader is referred to one of these previous studies for more information. Instrumental parameters associated with the Fourier Transform Spectrometer (FTS) used for the measurements, sample details, and the cell configuration are summarised in Table 2. The sample pressures and temperatures for each air-broadened spectrum, along with their experimental uncertainties and associated spectral resolutions, are listed in Table 3.

3.2. Generation of absorption cross sections

The procedure used to generate absorption cross sections from measured spectra has been reported previously (e.g. Harrison et al., 2010; Harrison, 2015b; Harrison, 2016), so the full details are not provided here. The wavenumber scale of the cross sections is calibrated

Manuscript under review for journal Atmos. Meas. Tech.

Discussion started: 22 May 2018

© Author(s) 2018. CC BY 4.0 License.





against the positions of isolated N₂O absorption lines taken from the HITRAN 2012 database (Rothman et al., 2013). The absorption cross sections, $\sigma(v, P_{air}, T)$ in units of cm² molecule⁻¹, at wavenumber v (cm⁻¹), temperature T (K) and synthetic air pressure P_{air} , are normalised according to

162
$$\int_{710 \,\mathrm{cm}^{-1}}^{1290 \,\mathrm{cm}^{-1}} \sigma(\nu, P_{air}, T) \partial \nu = 9.9515 \times 10^{-17} \,\mathrm{cm \, molecule^{-1}}, \tag{1}$$

where the value on the right hand side is the average integrated band intensity over the spectral range 710 – 1290 cm⁻¹ for three 760-Torr-N₂-broadened trichlorofluoromethane spectra (at 278, 298, and 323 K) from the Pacific Northwest National Laboratory (PNNL) IR database (Sharpe et al., 2004). This intensity calibration procedure counters problems with trichlorofluoromethane adsorption in the vacuum line and on the cell walls, and furthermore assumes that the integrated intensity over each band system is independent of temperature. The reader is referred to Harrison et al. (2010) for a more complete explanation of the underlying assumption, and references cited within Harrison (2015a, 2015b, and 2016) for details on previous successful uses of this approach.

A selection of the derived absorption cross sections is presented in Figure 2, showing the expected behaviour with temperature at a total pressure of ~ 200 Torr; the wavenumber range covers the microwindow for the ACE-FTS v3.6 retrieval scheme.

3.3. Absorption cross section uncertainties

The accuracy of the wavenumber scale for the new absorption cross sections is comparable to the accuracy of the N₂O lines used in the calibration; according to the HITRAN error codes, this is between 0.001 and 0.0001 cm⁻¹. The uncertainty in the intensity is dominated by systematic errors. A true measure of the random errors would ideally require multiple concentration-pathlength burdens at each PT combination, however only one is available for each. The maximum systematic uncertainties in the sample temperatures (μ_T) and total pressures (μ_P) are 0.4 % and 0.7 %, respectively (see Table 3). The photometric uncertainty (μ_{phot}), which includes systematic error arising from the use of Bruker's non-linearity correction for MCT detectors, is estimated to be ~2 %. The pathlength error (μ_{path}) is estimated to be negligibly small, lower than 0.1 %. According to the PNNL metadata, the systematic error in the PNNL CCl₃F spectra used for the intensity calibration is estimated to

Manuscript under review for journal Atmos. Meas. Tech.

Discussion started: 22 May 2018

© Author(s) 2018. CC BY 4.0 License.





be less than 3 % (2 σ). Equating the error, μ_{PNNL} , with the 1 σ value, i.e. 1.5 %, and assuming that the systematic errors for all the quantities are uncorrelated, the overall systematic error in the dataset can be given by:

193
$$\mu_{systematic}^2 = \mu_{PNNL}^2 + \mu_T^2 + \mu_P^2 + \mu_{phot}^2.$$
 (2)

Note that using PNNL spectra for intensity calibration effectively nullifies the errors in the trichlorofluoromethane partial pressures and cell pathlength, so these do not have to be included in Eq. 2. According to Eq. 2, the systematic error contribution, $\mu_{systematic}$, to the new cross sections is ~3% (1 σ).

4. Comparison between absorption cross-section datasets

In this section the new dataset presented in this work is compared with the older Varanasi dataset. The comparison focuses on their wavenumber scales, integrated band strengths, artefacts such as channel fringing, signal-to-noise ratios, spectral resolution, and PT coverage. In addition, the new dataset includes the weak combination band, $v_2 + v_5$, not present in the Varanasi measurements. This new dataset will be made available to the community via the HITRAN and GEISA databases, but in the meantime is available electronically from the author.

4.1. Wavenumber scale

It is likely that the wavenumber scale for the Varanasi dataset was never calibrated; this has been observed in a number of recent studies for other halogenated species in which new datasets have been compared with older Varanasi datasets, e.g. HFC-134a (Harrison, 2015a), CFC-12 (Harrison, 2015b), and HCFC-22 (Harrison, 2016). As explained earlier, the absolute accuracy of the wavenumber scale for the new dataset lies between 0.001 and 0.0001 cm⁻¹. In comparison, the v_4 band in the Varanasi cross sections is shifted too low in wavenumber; this shift varies between cross sections, e.g. by ~ 0.002 cm⁻¹ (a correction factor of ~ 1.000002) for the 190 K / 7.5 Torr v_1 Varanasi measurement and by ~ 0.007 cm⁻¹ (a correction factor of ~ 1.000007) for 216.1 K / 100.0 Torr v_1 .

4.2. Integrated band strengths

Manuscript under review for journal Atmos. Meas. Tech.

Discussion started: 22 May 2018







Integrated band strengths for the Varanasi cross sections have been calculated over the spectral ranges of the cross-section files, 810 – 880 and 1050 – 1120 cm⁻¹, covering the v4 and v1 bands respectively, and compared with those for the new absorption cross sections calculated over the same ranges; plots of integrated band strength against temperature for each dataset and wavenumber range can be found in Figure 3. At each temperature the Varanasi integrated band strengths display a small spread in values, most notably for the v4 band, however there is no evidence for any temperature dependence, as expected. The small spread in values is likely due to inconsistencies in the baselines for the Varanasi cross sections. Unfortunately, the wavenumber ranges do not extend far enough to obtain an unambiguous measure of the baseline position, and the cross sections in the HITRAN and GEISA databases have had all negative cross section values set to zero, which has the effect of adjusting the baseline positions by a small amount near the band wings.

4.3. Channel fringes

Most of the absorption cross sections in the Varanasi CFC-11 dataset contain noticeable channel fringes above the noise level (refer to Figure 4 for an example of this); in transmittance these would equate to peak-to-peak amplitudes as high as ~2–3 %. For the measurements described in the present work, wedged cell windows were used to avoid channel fringes by preventing reflections from components in the optical path of the spectrometer.

4.4. Signal-to-noise ratios (SNRs)

The SNRs of the transmittance spectra measured in the present work have been calculated using Bruker's OPUS software at ~ 990 cm⁻¹ where the transmittance is close to 1; the values range from 2600 to 4700 (rms), equivalent to percentage transmittances between 0.04 and 0.02 %. A direct comparison with the Varanasi dataset, however, is not possible without the original transmittance spectra or, at the very least, information on the experimental mixing ratios. Further complicating issues, the Varanasi cross sections are missing negative values near the baselines (refer to Section 4.2) and many have channel fringes superimposed. However, it is apparent from a direct inspection that the new cross sections have improved SNR, in some cases substantially so.

4.5. Spectral resolution

Manuscript under review for journal Atmos. Meas. Tech.

Discussion started: 22 May 2018

© Author(s) 2018. CC BY 4.0 License.





All spectra used to create the Varanasi cross-section dataset were either recorded at 0.01 (for sample mixtures of 75 Torr and below) or 0.03 cm⁻¹ spectral resolution (defined as 0.9/MOPD). In the present work 0.01 cm⁻¹ resolution was used for mixtures below 10 Torr, 0.03 cm⁻¹ for 300 Torr and above, and 0.015 and 0.0225 cm⁻¹ for intermediate pressures. The spectra recorded at 191.6 K and 98.14 / 200.0 Torr were mistakenly recorded at spectral resolutions of 0.0225 / 0.0300 cm⁻¹ instead of the planned 0.015 / 0.0225 cm⁻¹. However, careful inspection indicated that there was no under-resolving of spectral features for these two measurements. Overall, the dataset comparison indicates that the spectral resolutions chosen for the Varanasi measurements were suitable.

4.6. Pressure-temperature coverage

An absorption cross-section dataset used in remote sensing should cover all possible combinations of pressure and temperature appropriate for the region of the atmosphere being observed; in this case the focus is on the mid-troposphere (~ 5 km) up to the stratosphere. It is preferable to utilise an interpolation scheme in forward model calculations, rather than to extrapolate beyond the temperatures and pressures represented within the dataset. Figure 5 provides a graphical representation of the PT combinations for both datasets, illustrating the improved PT coverage (30 PT combinations in total) relative to the Varanasi dataset.

5. Conclusions

New high-resolution IR absorption cross sections for air-broadened trichlorofluoromethane (CFC-11) have been determined over the spectral range 710 - 1290 cm⁻¹, with an estimated systematic uncertainty of ~ 3 %. Spectra were recorded at resolutions between 0.01 and 0.03 cm⁻¹ (calculated as 0.9/MOPD) over a range of atmospherically relevant temperatures and pressures (7.5 – 760 Torr and 192 – 293 K). These new absorption cross sections improve upon those currently available in the HITRAN and GEISA databases. In particular, they cover a wider range of pressures and temperatures, they have a more accurately calibrated wavenumber scale, they have more consistent integrated band intensities, they do not display any channel fringing, they have improved SNR, and additionally they cover the weak combination band, $v_2 + v_5$.

Acknowledgements

Manuscript under review for journal Atmos. Meas. Tech.

Discussion started: 22 May 2018

321

© Author(s) 2018. CC BY 4.0 License.





The author wishes to thank the National Centre for Earth Observation (NCEO), 289 290 funded by the UK Natural Environment Research Council (NERC), for funding this work, as 291 well as R.G. Williams and R.A. McPheat for providing technical support during the 292 measurements. 293 294 **Figure Captions** 295 Figure 1. The absorption cross section of trichlorofluoromethane / dry synthetic air at 191.7 296 K and 7.535 Torr (this work), with vibrational band assignments for the main band systems in the $710 - 1290 \text{ cm}^{-1}$ spectral region. 297 298 299 Figure 2. The new absorption cross sections of trichlorofluoromethane / dry synthetic air at a 300 total pressure of ~ 200.0 Torr over a range of temperatures (191.6, 202.4, 216.6, 232.6, 301 252.5, and 273.8 K). The observed narrowing of the v₄ band as the temperature decreases is 302 due to the decline in Boltzmann populations of the upper rovibrational levels of the ground 303 state. 304 305 Figure 3. Integrated band strength as a function of temperature for the new and Varanasi 306 cross-section datasets over the wavenumber ranges 810 - 880 and 1050 - 1120 cm⁻¹. 307 308 Figure 4. The Varanasi absorption cross section of trichlorofluoromethane / dry synthetic air 309 at 232.7 K and 250.0 Torr (top), converted to transmittance by assuming similar sample 310 conditions to those in the present study. The resulting spectrum has been wavenumber 311 calibrated and divided by a transmittance spectrum interpolated between the new measured 312 spectra at 232.6 K and 201.0 / 399.8 Torr. Apart from the small difference arising from the 313 mis-match in sample conditions, the resulting ratio (bottom) indicates the presence of channel 314 fringes above the noise level. 315 316 Figure 5. A graphical representation of the PT coverage for both the new and Varanasi 317 datasets. 318 319 References 320 Bingham, G. E., Zhou, D. K., Bartschi, B. Y., Anderson, G. P., Smith, D. R., Chetwynd, J.

H., and Nadile, R. M.: Cryogenic Infrared Radiance Instrumentation for Shuttle (CIRRIS 1A)

Manuscript under review for journal Atmos. Meas. Tech.

Discussion started: 22 May 2018

© Author(s) 2018. CC BY 4.0 License.





- 322 earth limb spectral measurements, calibration, and atmospheric O₃, HNO₃, CFC-12, and
- 323 CFC-11 profile retrieval, J. Geophys. Res., 102, 3547–3558, 1997.

324

- 325 Brown, A. T., Chipperfield, M. P., Boone, C. D., Wilson, C., Walker, K. A., Bernath, P. F.:
- 326 Trends in atmospheric halogen containing gases since 2004, Journal of Quantitative
- 327 Spectroscopy and Radiative Transfer, 112, 2552-2566, 2011.

328

- 329 Carpenter, L.J. and Reimann, S. (Lead Authors), Burkholder, J.B., Clerbaux, C., Hall, B.D.,
- 330 Hossaini, R., Laube, J.C., and Yvon-Lewis, S.A.: Ozone-Depleting Substances (ODSs) and
- 331 Other Gases of Interest to the Montreal Protocol, Chapter 1 in Scientific Assessment of
- Ozone Depletion: 2014, Global Ozone Research and Monitoring Project Report No. 55,
- World Meteorological Organization, Geneva, Switzerland, 2014.

334

- Chang, A. Y., Salawitch, R. J., Michelsen, H. A., Gunson, M. R., Abrams, M. C., Zander, R.,
- Rinsland, C. P., Elkins, J. W., Dutton, G. S., Volk, C. M., Webster, C. R., May, R. D., Fahey,
- D. W., Gao, R.-S., Loewenstein, M., Podolske, J. R., Stimpfle, R. M., Kohn, D. W., Proffitt,
- 338 M. H., Margitan, J. J., Chan, K. R., Abbas, M. M., Goldman, A., Irion, F. W., Manney, G. L.,
- 339 Newchurch, M. J. and Stiller, G. P.: A comparison of measurements from ATMOS and
- instruments aboard the ER-2 aircraft: Halogenated gases, Geophysical Research Letters, 23,
- 341 2393-2396, 1996.

342

- 343 Dinelli, B. M., Arnone, E., Brizzi, G., Carlotti, M., Castelli, E., Magnani, L., Papandrea, E.,
- 344 Prevedelli, M., and Ridolfi, M.: The MIPAS2D database of MIPAS/ENVISAT
- 345 measurements retrieved with a multi-target 2-dimensional tomographic approach, Atmos.
- 346 Meas. Tech., 3, 355-374, doi:10.5194/amt-3-355-2010, 2010.

- 348 Gordon, I.E., Rothman, L.S., Hill, C., Kochanov, R.V., Tan, Y., Bernath, P.F., Birk, M.,
- 349 Boudon, V., Campargue, A., Chance, K.V., Drouin, B.J., Flaud, J.-M., Gamache, R.R.,
- 350 Hodges, J.T., Jacquemart, D., Perevalov, V.I., Perrin, A., Shine, K.P., Smith, M.-A.H.,
- Tennyson, J., Toon, G.C., Tran, H., Tyuterev, .G., Barbe, A., Császár, A.G., Devi, V.M.,
- 352 Furtenbacher, T., Harrison, J.J., Hartmann, J.-M., Jolly, A., Johnson, T.J., Karman, T.,
- 353 Kleiner, I., Kyuberis, A.A., Loos, J., Lyulin, O.M., Massie, S.T., Mikhailenko, S.N.,
- 354 Moazzen-Ahmadi, N., Müller, H.S.P., Naumenko, O.V., Nikitin, A.V., Polyansky, O.L., Rey,
- 355 M., Rotger, M., Sharpe, S.W., Sung, K., Starikova, E., Tashkun, S.A., Vander Auwera, J.,

Manuscript under review for journal Atmos. Meas. Tech.

Discussion started: 22 May 2018

© Author(s) 2018. CC BY 4.0 License.





- 356 Wagner, G., Wilzewski, J., Wcisło, P., Yu, S., Zak, E.J.: The HITRAN2016 molecular
- 357 spectroscopic database, Journal of Quantitative Spectroscopy and Radiative Transfer, in
- 358 press, 2017, doi:10.1016/j.jqsrt.2017.06.038.

359

- 360 Harris, N.R.P. and Wuebbles, D.J. (Lead Authors), Daniel, J.S., Hu, J., Kuijpers, L.J.M.,
- 361 Law, K.S., Prather, M.J., and Schofield, R.: Scenarios and information for policymakers,
- 362 Chapter 5 in Scientific Assessment of Ozone Depletion: 2014, Global Ozone Research and
- 363 Monitoring Project Report No. 55, World Meteorological Organization, Geneva,
- 364 Switzerland, 2014.

365

- 366 Harrison, J.J., Allen. N.D.C., Bernath, P.F.: Infrared absorption cross sections for ethane
- 367 (C₂H₆) in the 3 µm region, Journal of Quantitative Spectroscopy and Radiative Transfer, 111,
- 368 357-363, doi: 10.1016/j.jgsrt.2009.09.010, 2010.

369

- 370 Harrison, J.J.: Infrared absorption cross sections for 1,1,1,2-tetrafluoroethane, Journal of
- 371 Quantitative Spectroscopy and Radiative Transfer, 151, 210–216,
- 372 doi:10.1016/j.jqsrt.2014.09.023, 2015a.

373

- 374 Harrison, J.J.: New and improved infrared absorption cross sections for
- dichlorodifluoromethane (CFC-12), Atmos. Meas. Tech., 8, 3197-3207, doi:10.5194/amt-8-
- 376 3197-2015, 2015b.

377

- 378 Harrison, J. J.: New and improved infrared absorption cross sections for
- 379 chlorodifluoromethane (HCFC-22), Atmos. Meas. Tech., 9, 2593-2601, doi:10.5194/amt-9-
- 380 2593-2016, 2016.

381

- 382 Hoffmann, L., Spang, R., Kaufmann, M., and Riese, M.: Retrieval of CFC-11 and CFC-12
- 383 from Envisat MIPAS observations by means of rapid radiative transfer calculations, Adv.
- 384 Space Res., 36, 915-921, doi:10.1016/j.asr.2005.03.112, 2005.

- 386 Hoffmann, L., Hoppe, C. M., Müller, R., Dutton, G. S., Gille, J. C., Griessbach, S., Jones, A.,
- 387 Meyer, C. I., Spang, R., Volk, C. M., and Walker, K. A.: Stratospheric lifetime ratio of CFC-
- 388 11 and CFC-12 from satellite and model climatologies, Atmos. Chem. Phys., 14, 12479-
- 389 12497, doi:10.5194/acp-14-12479-2014, 2014.

Manuscript under review for journal Atmos. Meas. Tech.

Discussion started: 22 May 2018

© Author(s) 2018. CC BY 4.0 License.





390

- 391 Irion F.W., Gunson M.R., Toon G.C., Chang A.Y., Eldering A., Mahieu E., Manney G.L.,
- 392 Michelsen H.A., Moyer E.J., Newchurch M.J., Osterman G.B., Rinsland C.P., Salawitch R.J.,
- 393 Sen B., Yung Y.L., Zander R., Atmospheric Trace Molecule Spectroscopy (ATMOS)
- Experiment Version 3 data retrievals, Applied Optics, 41, 6968-6979, 2002.

395

- 396 Jacquinet-Husson, N., Armante, R., Scott, N.A., Chédin, A., Crépeau, L., Boutammine, C.,
- 397 Bouhdaoui, A., Crevoisier, C., Capelle, V., Boonne, C., Poulet-Crovisier, N., Barbe, A.,
- 398 Benner, D.C., Boudon, V., Brown, L.R., Buldyreva, J., Campargue, A., Coudert, L.H., Devi,
- 399 V.M., Down, M.J., Drouin, B.J., Fayt, A., Fittschen, C., Flaud, J.-M., Gamache, R.R.,
- 400 Harrison, J.J., Hill, C., Hodnebrog, Ø., Hu, S.-M., Jacquemart, D., Jolly, A., Jiménez, E.,
- 401 Lavrentieva, N.N., Liu, A.-W., Lodi, L., Lyulin, O.M., Massie, S.T., Mikhailenko, S., Müller,
- 402 H.S.P., Naumenko, O.V., Nikitin, A., Nielsen, C.J., Orphal, J., Perevalov, V.I., Perrin, A.,
- 403 Polovtseva, E., Predoi-Cross, A., Rotger, M., Ruth, A.A., Yu, S.S., Sung, K., Tashkun, S.A.,
- 404 Tennyson, J., Tyuterev, Vl.G., Vander Auwera, J., Voronin, B.A., Makie, A., The 2015
- 405 edition of the GEISA spectroscopic database, Journal of Molecular Spectroscopy, 327, 31-72,
- 406 doi: 10.1016/j.jms.2016.06.007, 2016.

407

- 408 Kellmann, S., von Clarmann, T., Stiller, G. P., Eckert, E., Glatthor, N., Höpfner, M., Kiefer,
- 409 M., Orphal, J., Funke, B., Grabowski, U., Linden, A., Dutton, G. S., and Elkins, J. W.: Global
- 410 CFC-11 (CCl3F) and CFC-12 (CCl2F2) measurements with the Michelson Interferometer for
- 411 Passive Atmospheric Sounding (MIPAS): retrieval, climatologies and trends, Atmos. Chem.
- 412 Phys., 12, 11857–11875, doi:10.5194/acp-12-11857-2012, 2012.

413

- 414 Li, Z., and Varanasi, P.: Measurement of the absorption cross-sections of CFC-11 at
- 415 conditions representing various model atmospheres, Journal of Quantitative Spectroscopy
- 416 and Radiative Transfer, 52, 137-144, 1994.

417

- 418 Massie, S. T. and Goldman, A.: Absorption parameters of very dense molecular spectra for
- 419 the HITRAN compilation, Journal of Quantitative Spectroscopy and Radiative Transfer, 48,
- 420 713-719, 1992.

Manuscript under review for journal Atmos. Meas. Tech.

Discussion started: 22 May 2018

© Author(s) 2018. CC BY 4.0 License.





- 422 Massie, S. T., Goldman, A., Murcray, D. G., and Gille, J. C.: Approximate absorption cross-
- 423 sections of F12, F11, ClONO₂, N₂O₅, HNO₃, CCl₄, CF₄, F21, F113, F114, and HNO₄, Appl.
- 424 Opt. 24, 3426-3427, 1985.

425

- 426 McDaniel, A. H., Cantrell, C. A., Davidson, J. A., Shetter, R. E., and Calvert, J. G.: The
- 427 Temperature Dependent, Infrared Absorption Cross-Sections for the Chlorofluorocarbons:
- 428 CFC-11, CFC-12, CFC-13, CFC-14, CFC-22, CFC-113, CFC-114, and CFC-115, Journal of
- 429 Atmospheric Chemistry, 12, 211-227, 1991.

430

- 431 Offermann, D., Grossmann, K.-U., Barthol, P., Knieling, P., Riese, M., and Trant, R.:
- 432 Cryogenic Infrared Spectrometers and Telescopes for the Atmosphere (CRISTA) experiment
- 433 and middle atmosphere variability, J. Geophys. Res., 104, 16311-16325,
- 434 doi:10.1029/1998JD100047, 1999.

435

- 436 Roche, A.E., Kumer, J.B., Mergenthaler, J.L., Ely, G.A., Uplinger, W.G., Potter, J.F., James,
- 437 T.C., Sterritt, L.W.: The cryogenic limb array etalon spectrometer (CLAES) on UARS:
- 438 Experiment description and performance, J. Geophys. Res., 98(D6), 10763-10775, 1993,
- 439 doi:10.1029/93JD00800.

440

- 441 Rothman, L.S., Gamache, R.R., Goldman, A., Brown, L.R., Toth, R.A., Pickett, H.M.,
- 442 Poynter, R.L., Flaud, J.-M., Camy-Peyret, C., Barbe, A., Husson, N., Rinsland, C.P., and
- 443 Smith, M.A.H.: The HITRAN database: 1986 edition, Appl. Opt., 26, 4058-4097, 1987.

444

- 445 Rothman, L.S., Gamache, R.R., Tipping, R.H., Rinsland, C.P., Smith, M.A.H., Benner D. C.,
- 446 Devi, V.M, Flaud, J.-M., Camy-Peyret, C., Perrin, A., Goldman, A., Massie, S.T., Brown,
- 447 L.R., Toth, R.A.: The HITRAN molecular database: Editions of 1991 and 1992, Journal of
- 448 Quantitative Spectroscopy and Radiative Transfer, 48, 469–507, 1992.

- 450 Rothman, L.S., Rinsland, C.P., Goldman, A., Massie, S.T., Edwards, D.P., Flaud, J-M.,
- 451 Perrin, A., Camy-Peyret, C., Dana, V., Mandin, J.-Y., Schroeder, J., Mccann, A., Gamache,
- 452 R.R., Wattson, R.B., Yoshino, K., Chance, K.V., Jucks, K.W., Brown, L.R., Nemtchinov, V.,
- 453 Varanasi, P.: The HITRAN Molecular Spectroscopic Database and Hawks (HITRAN
- 454 Atmospheric Workstation): 1996 Edition, Journal of Quantitative Spectroscopy and
- 455 Radiative Transfer, 60, 665-710, 1998.

Manuscript under review for journal Atmos. Meas. Tech.

Discussion started: 22 May 2018

464

474

478

482

486

© Author(s) 2018. CC BY 4.0 License.





456
457 Rothman, L.S., Barbe, A., Benner, D.C., Brown, L.R., Camy-Peyret, C., Carleer, M.R.,

Chance, K., Clerbaux, C., Dana, V., Devi, V.M., Fayt, A., Flaud, J.-M., Gamache, R.R.,

459 Goldman, A., Jacquemart, D., Jucks, K.W., Lafferty, W.J., Mandin, J.-Y., Massie, S.T.,

Nemtchinov, V., Newnham, D.A., Perrin, A., Rinsland, C.P., Schroeder, J., Smith, K.M.,

461 Smith, M.A.H., Tang, K., Toth, R.A., Vander Auwera, J., Varanasi, P., Yoshino, K.: The

462 HITRAN molecular spectroscopic database: Edition of 2000 including updates through 2001,

Journal of Quantitative Spectroscopy and Radiative Transfer, 82, 5-44, 2003.

Rothman, L.S., Gordon, I.E., Babikov, Y., Barbe, A., Benner, D.C., Bernath, P.F., Birk, M.,

466 Bizzocchi, L., Boudon, V., Brown, L.R., Campargue, A., Chance, K., Cohen, E.A., Coudert,

467 L.H., Devi, V.M., Drouin, B.J., Fayt, A., Flaud, J.-M., Gamache, R.R., Harrison, J.J.,

468 Hartmann, J.-M., Hill, C., Hodges, J.T., Jacquemart, D., Jolly, A., Lamouroux, J., Le Roy,

469 R.J., Li, G., Long, D.A., Lyulin, O.M., Mackie, C.J., Massie, S.T., Mikhailenko, S., Müller,

470 H.S.P., Naumenko, O.V., Nikitin, A.V., Orphal, J., Perevalov, V., Perrin, A., Polovtseva,

471 E.R., Richard, C., Smith, M.A.H., Starikova, E., Sung, K., Tashkun, S., Tennyson, J., Toon,

472 G.C., Tyuterev, Vl.G., Wagner, G.: The HITRAN2012 molecular spectroscopic database,

Journal of Quantitative Spectroscopy and Radiative Transfer, 130, 4-50, 2013.

475 Sharpe, S.W., Johnson, T.J., Sams, R.L., Chu, P.M., Rhoderick, G.C. and Johnson, P.A.:

476 Gas-phase databases for quantitative infrared spectroscopy, Applied Spectroscopy, 58, 1452-

477 61, 2004.

479 Snels, M., D'Amico, G., Piccarreta, L., Hollenstein, H. and Quack, M.: Diode-Laser Jet

480 Spectra and Analysis of the v₁ and v₄ Fundamentals of CCl₃F, J. Mol. Spectrosc., 205, 102–

481 109, 2001.

483 von Lilienfeld, O.A., Leonard, C., Handy, N.C., Carter, S., Willeke, M. and Quack, M.:

484 Spectroscopic properties of trichlorofluoromethane CCl₃F calculated by density functional

485 theory, Phys. Chem. Chem. Phys., 9, 5027–5035, doi: 10.1039/B704995A, 2007.

487 Wetzel, G., Oelhaf, H., Friedl-Vallon, F., Kleinert, A., Lengel, A., Maucher, G., Nordmeyer,

488 H., Ruhnke, R., Nakajima, H., Sasano, Y., Sugita, T., and Yokota, T.: Intercomparison and

Manuscript under review for journal Atmos. Meas. Tech.

Discussion started: 22 May 2018

© Author(s) 2018. CC BY 4.0 License.





489 validation of ILAS-II version 1.4 target parameters with MIPAS-B measurements, J.

490 Geophys. Res., 111, D11S06, doi:10.1029/2005JD006287, 2006.

491

492 Yokota, T., Nakajima, H., Sugita, T., Tsubaki, H., Itou, Y., Kaji, M., Suzuki, M., Kanzawa,

493 H., Park, J.H., Sasano, Y.: Improved Limb Atmospheric Spectrometer (ILAS) data retrieval

494 algorithm for Version 5.20 gas profile products, J. Geophys. Res., 107(D24), 8216,

495 doi:10.1029/2001JD000628, 2002.

496

497 498

Tables

499

Table 1: Summary of limb sounders past and present capable of measuring CFC-11.

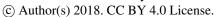
Instrument	Platform	
` 1	Space shuttle	Chang et al., 1996;
MOlecule Spectroscopy)		Irion et al., 2002
CIRRIS 1A (Cryogenic InfraRed	Space shuttle	Bingham et al., 1997
Radiance Instrumentation for Shuttle)		
CRISTA (CRyogenic Infrared	Space shuttle	Offermann et al., 1999
Spectrometers and Telescopes for the		
Atmosphere)		
CLAES (Cryogenic Limb Array	UARS (Upper Atmosphere	Roche, et al., 1993
Etalon Spectrometer)	Research Satellite)	
ILAS (Improved Limb Atmospheric	ADEOS (ADvanced Earth	Yokota, et al., 2002
Spectrometer)	Observing Satellite)	
ILAS II	ADEOS II	Wetzel et al., 2006,
HIRDLS (HIgh Resolution Dynamics	Aura	Hoffmann et al., 2014
Limb Sounder)		
MIPAS (Michelson Interferometer for	ENVISAT	e.g. Hoffmann et al., 2005;
Passive Atmospheric Sounding)	(ENVIronmental	Dinelli et al., 2010;
	SATellite)	Kellmann et al., 2012
ACE-FTS (Atmospheric Chemistry	SCISAT	Brown et al., 2011
Experiment – Fourier transform		
spectrometer)		

501

502

Manuscript under review for journal Atmos. Meas. Tech.

Discussion started: 22 May 2018







504	Table 2: FTS parameters, sample conditions, and cell configuration for all measurements			
	Spectrometer	Bruker Optics IFS 125HR		
	Mid-IR source	Globar		
	Detector	Mercury cadmium telluride (MCT) D313 ^a		
	Beam splitter	Potassium bromide (KBr)		
	Optical filter	~700–1400 cm ⁻¹ bandpass		
	Spectral resolution	0.01 to 0.03 cm ⁻¹		
	Aperture size	3.15 mm		
	Apodisation function	Boxcar		
	Phase correction	Mertz		
	CCl ₃ F (Supelco)	99.9% purity, natural-abundance isotopic mixture; freeze-pump-		
		thaw purified multiple times prior to use		
	Air zero (BOC Gases)	total hydrocarbons < 3 ppm, H2O < 2 ppm, CO2 < 1 ppm, CO < 1		
		ppm; used 'as is'		
	Cell pathlength	26 cm		
	Cell windows	Potassium bromide (KBr) (wedged)		
	Pressure gauges	3 MKS-690A Baratrons (1, 10 & 1000 Torr) (±0.05% accuracy)		
	Refrigeration	Julabo F95-SL Ultra-Low Refrigerated Circulator (with ethanol)		
	Thermometry	4 PRTs, Labfacility IEC 751 Class A		
	Wavenumber calibration	N_2O		
505 506 507 508	^a Due to the non-linear response of MCT detectors to the detected radiation, all interferograms were Fourier transformed using Bruker's OPUS software with a non-linearity correction applied.			

Manuscript under review for journal Atmos. Meas. Tech.

Discussion started: 22 May 2018

© Author(s) 2018. CC BY 4.0 License.





Table 3: Summary of the sample conditions for all measurements.

Temperature (K)	Initial CCl ₃ F	Total Pressure (Torr)	Spectral resolution
	Pressure (Torr) ^a		$({\rm cm}^{-1})^b$
191.7 ± 0.8	0.266	7.535 ± 0.035	0.0100
191.5 ± 0.8	0.302	49.83 ± 0.13	0.0150
191.6 ± 0.8	0.302	98.14 ± 0.68	0.0225
191.6 ± 0.8	0.266	200.0 ± 0.3	0.0300
202.3 ± 0.5	0.319	7.508 ± 0.006	0.0100
202.4 ± 0.5	0.309	50.28 ± 0.13	0.0150
202.3 ± 0.5	0.318	99.85 ± 0.30	0.0150
202.4 ± 0.5	0.309	200.4 ± 0.2	0.0225
202.3 ± 0.5	0.318	301.6 ± 0.3	0.0300
216.7 ± 0.5	0.347	7.496 ± 0.018	0.0100
216.7 ± 0.5	0.358	49.93 ± 0.09	0.0150
216.7 ± 0.5	0.357	99.94 ± 0.07	0.0150
216.6 ± 0.5	0.375	201.0 ± 0.2	0.0225
216.7 ± 0.5	0.383	360.4 ± 0.3	0.0300
232.6 ± 0.4	0.407	7.500 ± 0.020	0.0100
232.6 ± 0.4	0.395	49.80 ± 0.15	0.0150
232.6 ± 0.4	0.544	99.67 ± 0.16	0.0150
232.6 ± 0.4	0.417	201.0 ± 0.1	0.0225
232.6 ± 0.4	0.413	399.8 ± 0.3	0.0300
252.5 ± 0.2	0.503	7.477 ± 0.003	0.0100
252.5 ± 0.2	0.486	50.06 ± 0.05	0.0150
252.5 ± 0.2	0.516	200.9 ± 0.1	0.0225
252.5 ± 0.2	0.544	399.9 ± 0.2	0.0300
252.5 ± 0.2	0.607	600.2 ± 0.3	0.0300
273.9 ± 0.2	0.475	7.501 ± 0.001	0.0100
273.8 ± 0.2	0.613	201.6 ± 0.1	0.0225
273.8 ± 0.2	0.598	355.8 ± 0.1	0.0300
273.8 ± 0.2	0.607	760.1 ± 0.2	0.0300
293.1 ± 0.1	0.548	355.8 ± 0.1	0.0300
293.0 ± 0.1	0.566	760.0 ± 0.1	0.0300

⁵¹¹ a MKS-690A Baratron readings are accurate to \pm 0.05%.

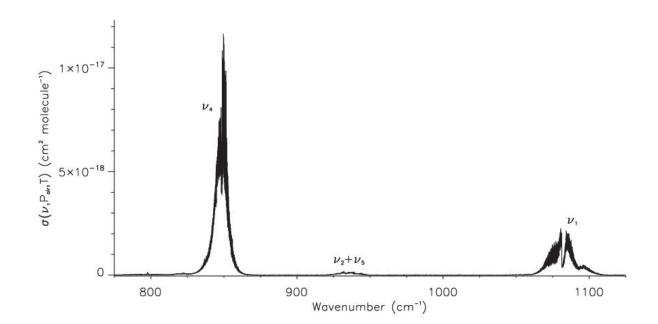
^{512 &}lt;sup>b</sup> Using the Bruker definition of 0.9/MOPD.

Atmos. Meas. Tech. Discuss., https://doi.org/10.5194/amt-2018-51 Manuscript under review for journal Atmos. Meas. Tech. Discussion started: 22 May 2018

© Author(s) 2018. CC BY 4.0 License.





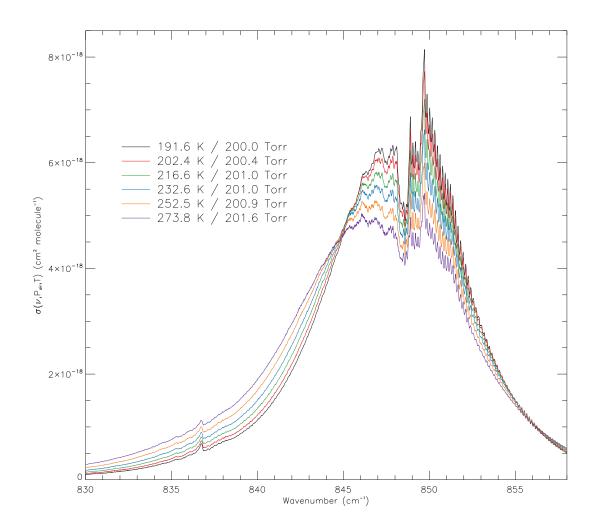


Atmos. Meas. Tech. Discuss., https://doi.org/10.5194/amt-2018-51 Manuscript under review for journal Atmos. Meas. Tech. Discussion started: 22 May 2018

© Author(s) 2018. CC BY 4.0 License.



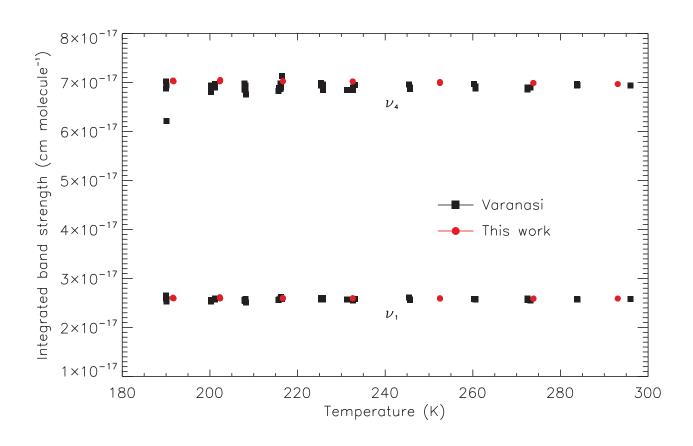




Atmos. Meas. Tech. Discuss., https://doi.org/10.5194/amt-2018-51 Manuscript under review for journal Atmos. Meas. Tech. Discussion started: 22 May 2018 © Author(s) 2018. CC BY 4.0 License.







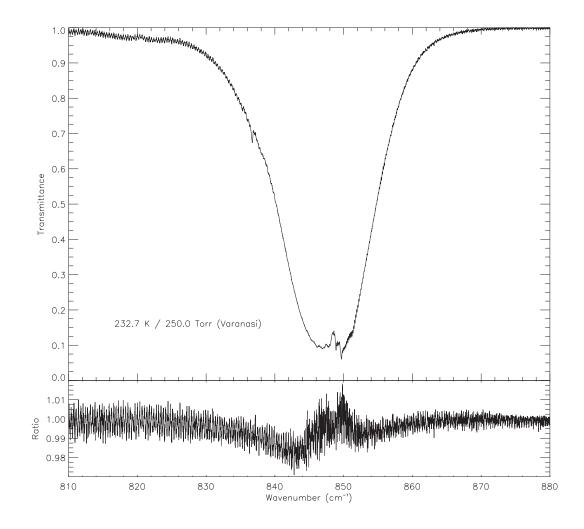
Atmos. Meas. Tech. Discuss., https://doi.org/10.5194/amt-2018-51 Manuscript under review for journal Atmos. Meas. Tech.

Discussion started: 22 May 2018

© Author(s) 2018. CC BY 4.0 License.







Atmos. Meas. Tech. Discuss., https://doi.org/10.5194/amt-2018-51 Manuscript under review for journal Atmos. Meas. Tech. Discussion started: 22 May 2018 © Author(s) 2018. CC BY 4.0 License.





